Available online at www.sciencedirect.com

ScienceDirect

Ceramics International 39 (2013) 8781–8787

CERAMICS INTERNATIONAL

www.elsevier.com/locate/ceramint

# Effects of foam composition on the microstructure and piezoelectric properties of macroporous PZT ceramics from ultrastable particle-stabilized foams

Wei Liu[a,*], Linjing Du[a], Yanzhong Wang[a], Jinlong Yang[a,b,**], Hong Xu[a]

[a]School of Materials Science and Engineering, North University of China, Taiyuan 030051, China
[b]State Key Lab of New Ceramics and Fine Processing, School of Materials Science and Engineering, Tsinghua University, Beijing 100084, China

Received 26 February 2013; received in revised form 17 April 2013; accepted 18 April 2013
Available online 23 April 2013

**Abstract**

Porous lead zirconate titanate (PZT) ceramics could be produced by combining the particle-stabilized foams and the gelcasting technique. In this study, the foaming capacity of particle-stabilized wet foams was tailored by changing the concentration of valeric acid and pH values of suspension. Accordingly, porous PZT ceramics with different porosity, microstructure, dielectric and piezoelectric properties were prepared with the respective wet foam. Increase in the porosity led to a reduction in the relative permittivity ($\varepsilon_r$), a moderate decline in the longitudinal piezoelectric strain coefficient ($d_{33}$) and a rapid decline in the transverse piezoelectric strain coefficient ($d_{31}$), which endowed porous PZT ceramics with a high value of hydrostatic strain coefficient ($d_h$) and hydrostatic figure of merit (HFOM). As a result, the prepared samples possessed a maximal HFOM value of $19{,}520 \times 10^{-15}$ $Pa^{-1}$ with the porosity of 76.3%. The acoustic impedance ($Z$) of specimens had the lowest value of 1.35 Mrayl, which could match well with those of water or biological tissue; accordingly, the material would be beneficial in underwater sonar detectors or medical ultrasonic imaging.


*Keywords:* A. Particle-stabilized foams; C. Dielectric properties; C. Piezoelectric properties; D. PZT

## 1. Introduction

Lead zirconate titanate (PZT) has been extensively used for a host of sensor and actuator applications for its excellent piezoelectric properties [1–3]. However, for low frequency hydrophone application (10–100 kHz), underwater transducers, and biomedical imaging etc., porous PZT composites are preferred for low density, improved acoustic matching with water, high hydrostatic coefficients, and high hydrostatic figure of merit (HFOM). Generally, porous PZT composites could be classified into PZT/polymer and PZT/air (porous PZT ceramic). Compared with the PZT/polymer composites, porous PZT ceramics possess numerous advantages, such as brief manufacturing procedure, broad usage temperature, and roughly linear relationship between the piezoelectric properties and porosity [4]. In recent years, porous PZT ceramics have been developed using various processing techniques such as the lost wax replication of a coral skeleton [5], carbon fabrics [6], mixing of burnable plastic spheres (BURPS) processes [7], gelcasting [8], etc. Each process leads to the formation of its own microstructure and properties with varied porosities.

Due to the simplicity, versatility and low cost, the direct foaming technique is always of great interest to produce porous ceramics [9]. In this method, air bubbles are incorporated into a ceramic suspension by mechanical frothing to produce wet foams. Then the foams are dried and sintered to obtain high-strength porous ceramics. However, wet foams are thermodynamically unstable systems which undergo continuous Ostwald ripening and coalescence processes in order to decrease the foam overall free energy, so the wet foams are usually stabilized by long-chain surfactants or by colloidal particles. Recently, a sort of ultra-stable wet foams was utilized

*Corresponding author. Tel./fax: +86 351 3559638.
**Corresponding author at: State Key Lab of New Ceramics and Fine Processing, School of Materials Science and Engineering, Tsinghua University, Beijing 100084, China.
*E-mail addresses:* lwnuc@163.com (W. Liu), jlyang@mail.tsinghua.edu.cn (J. Yang).

0272-8842/$ - see front matter © 2013 Elsevier Ltd and Techna Group S.r.l. All rights reserved.
http://dx.doi.org/10.1016/j.ceramint.2013.04.065

to produce porous ceramics [10,11]. In the method, partial hydrophobization is first achieved by modifying the ceramic particle surface with short-chain carboxylic acids that adsorb with the carboxylate group onto particles, leaving the hydrophobic tail in contact with the aqueous solution. Then the modified particles adsorb onto the air–water interface of freshly incorporated air bubbles and reduce the foam overall free energy by removing part of the highly energetic gas–liquid interfacial area to form ultra-stable wet foams. The stability of wet foams is mainly determined by the surface properties of the resulting modified particles, which can be affected by the concentration of adsorbed amphiphilic molecules or the pH value of suspension.

In order to fabricate solid porous PZT ceramics from particle-stabilized wet foams, shaping, drying, and sintering have to be accomplished. Gelcasting, first developed by Omatete and Janney during the 1990s, has been applied not only to the fabrication of dense ceramics, but also to porous ceramics and complex-shaped ceramic parts [12–15]. The gelcasting process involves a suspension of ceramic powders in an aqueous monomer solution creating a 3D network by in situ polymerization, which holds ceramic powders in the shape of the mold cavity.

Our group, recently, successfully produced porous PZT ceramics with excellent piezoelectric properties by combining the particle-stabilized foams and the gelcasting technique [16]. However, there have been few investigations carried out to understand the effects of foam composition on the properties of porous PZT ceramics. In the present work, the concentration of adsorbed amphiphilic molecules and pH values of final suspension were investigated for structural, dielectric, and piezoelectric properties such as foaming capacity, density, microstructures, relative permittivity, etc.

## 2. Experimental procedure

### 2.1. Materials

PZT-5H powders (BaoDing HongSheng Acoustics Electron Apparatus Co. Ltd., Hebei Province, China) with a mean particle size of 1.87 μm and a density of 7.6 g/cm$^3$ were employed in the experiment. Valeric acid ($C_5H_{10}O_2$, Sinopharm Chemical Reagent Co., Ltd., Shanghai, China) was selected for the short-chain amphiphilic molecules to hydrophobize the particle surface. Acrylamide (AM, $C_2H_3CONH_2$) and *N*,*N*′-methylenebisacrylamide (MBAM, $(C_2H_3CONH)_2CH_2$) were selected as the organic monomers. Ammonium persulfate solution (APS, $(NH_4)_2S_2O_8$, 35 wt%) as an initiator and *N*,*N*, *N*′,*N*′-tetramethylenediamine (TEMED) as a catalyst were employed for the gelation process.

### 2.2. Sample preparation

Suspensions containing valeric acid were produced as follows: a premix solution of monomers was prepared by adding into deionized water AM and MBAM with concentrations of 14.5 wt% and 0.5 wt% respectively, then PZT powder was added stepwise to the solution to obtain a suspension with a solid loading of 15 vol%. Homogenization and deagglomeration were carried out on a ball mill for 4 h. An aqueous solution containing valeric acid was then slowly added dropwise to the ball-milled slurry under slight stirring to avoid local particle agglomeration. The concentration of valeric acid was determined by PZT suspension and set to 10, 30, 50, 70 and 90 mmol/L in this research. Afterward, the pH was set to its desired value (pH = 1, 3, 5, 7 and 9) employing HCl aqueous solution. In order to minimize the influence of water brought in by HCl solution, different concentrations of HCl aqueous solution (1, 3 and 5 mol/L) were employed in the experiment. Then the slurry was ball-milled again for 4 h to enable valeric acid to modify the surface of PZT particles sufficiently.

Foaming of suspensions was carried out using a household mixer at 300 r/min for 5 min. Meanwhile, the catalyst and initiator were added to the particle-stabilized foams with the amounts of 0.5 vol% and 1 vol% respectively; then the polymerization of AM started with an obvious increase in temperature in several minutes. The wet foams were then cast into a mold while in situ polymerization continued. After about 12 h, wet green parts were removed from the mold and dried at 40 °C. The dried bodies, which had no obvious shrinkage in the drying process, were subsequently sintered in a corundum crucible containing $PbZrO_3$ powder to produce an excess PbO atmosphere at 1150 °C for 2 h.

### 2.3. Characterization

Each test in our research led to 3–4 samples and all samples were subjected to simple machining to be disc-shaped with a typical size of 10 mm in diameter and 1.5 mm in height. The porosity of sintered sample was obtained from the ratio of the measured bulk density, measured by using the water displacement method based on the Archimedean principles, to the theoretical one of this PZT material (7.6 g/cm$^3$). The microstructures of porous PZT ceramics were observed using SSX-550 scanning electron microscopy (SHIMAZU, Shimazu Corp., Kyoto, Japan). Cell size was measured from the obtained SEM photographs using the image analysis software (Image J) [17]. For dielectric and piezoelectric testing, both surfaces of the samples were coated with a thin silver layer, followed by heat treatment at around 550 °C for 20 min to form electrodes. To minimize the penetration of silver into porous ceramic bodies, the silver paste was made highly viscous by adding ethyl cellulose (EC). Thereafter, the samples were poled by applying a dc field of 10 kV/cm for 10 min in a bath of silicone oil at 120 °C, and subsequently aged for 24 h before testing. The longitudinal piezoelectric strain coefficient ($d_{33}$) was measured by a direct method based on a Quasti-static $d_{33}$-meter (ZJ-3A, Institute of Acoustics, Chinese Academy of Science, Beijing, China). The relative permittivity ($\varepsilon_r$) was calculated from the capacitance by the formula

$$\varepsilon_r = \left(\frac{1}{\varepsilon_0}\right)\frac{C_0 d}{S} \quad (1)$$

where $\varepsilon_0$ is the vacuum permittivity, $C_0$ the capacitance at 1 kHz measured under constant (zero) stress by using an

impedance bridge (HP-4194A, Hewlett-Packard Development Company, CA), $d$ the thickness of the porous PZT disk and $S$ is the area of the electrode. The transverse piezoelectric strain coefficient ($d_{31}$) was determined from the values of resonant and anti-resonant vibration frequencies, density, diameter and dielectric constant. The parameters hydrostatic strain coefficient ($d_h = d_{33} + 2d_{31}$), hydrostatic voltage coefficient ($g_h = d_h/\varepsilon_0\varepsilon_r$), hydrostatic figure of merit (HFOM $= d_h g_h$) and acoustic impedance ($Z$) were calculated from the measured values and other physical parameters.

## 3. Results and discussion

It should be noted that wet foams investigated in this study are quite complex systems. A series of situations are involved in the stabilization process, including the adsorption of short-chain amphiphilic molecules on the particle surface, and the adsorption of in situ-hydrophobized ceramic powders to the air–water interface of freshly air bubbles. Therefore, changes in the initial composition of suspension often affect more than one of the parameters relevant for foam formation and stabilization. In this paper, two important parameters, the concentration of valeric acid and pH value of the final slurry, were investigated independently.

### 3.1. Porosity and microstructures

Fig. 1 shows the effect of valeric acid concentration on the foaming capacity and hence the bulk density of sintered specimens. All measurements were carried out in suspensions containing 15 vol% PZT at pH 5.

As shown in Fig. 1, there is a distinct increase in the foaming capacity (the ratio of foam volume to slurry volume) from 1.68 to 2.93 with the increase of the valeric acid concentration. When the concentration of valeric acid was less than 30 mmol/L, the number of amphiphilic molecules was not enough to adsorb to ceramic particles, which degraded directly the hydrophobicity of colloidal particles and led to a relatively low foaming capacity of the suspension. With increasing the valeric acid concentration, there was a higher adsorption of amphiphilic molecules onto particles, the hydrophobicity of particles to adsorb to air–water interfaces was enhanced, resulting in stable wet foams and an increasing foaming capacity up to 2.93. Accordingly, the bulk density of porous ceramics decreased almost linearly from 4.16 g/cm$^3$ to 1.80 g/cm$^3$ in the range of valeric acid concentration, indicating that the density could be easily tailored in a broad range.

Besides the valeric acid concentration, pH value of the slurry also influences the stabilization of wet foams. Fig. 2 shows the effect of pH value on the foaming capacity and the bulk density of porous ceramics. Here, all measurements were carried out in suspensions with solid loading of 15 vol%, and the amount of valeric acid corresponded to a constant concentration of 50 mmol/L.

As depicted in Fig. 2, the foaming capacity shows a moderate increase from 1.96 to 2.46 upon increasing the pH value from 1 to 5. Obviously, when the pH value was below 5, substantive ionized $H^+$ in the acid suspension prevented the ionization of the valeric acid anion, which degraded the modification of amphiphilic molecules on PZT particles. When the pH value approached the isoelectric point of PZT colloids (pH 6.5–7) [18], the viscosity of the initial suspension increased, the particles tended to agglomerate, and the foaming capacity decreased to 1.76 consequently. Under mild alkaline condition (pH 9), valeric acid anion was hard to ionize, resulting in the lowest foaming capacity of 1.32. Meanwhile, the bulk density of samples varied between 2.38 and 5.09 g/cm$^3$ with a changing trend opposite to that of foaming capacity.

Fig. 3 shows the detailed pore morphology and interconnection of sintered porous ceramics with different initial compositions. As shown in Fig. 3(a), cells were mostly closed with an average size of approximately 223 μm, and separated from each other by particle walls with thicknes around 30 μm. In this case, the modified particles could cover most air bubbles of wet foams due to the cause of relatively small total volume of wet foams, and the coverage remained throughout the gelling, drying and sintering procedure, leading to the

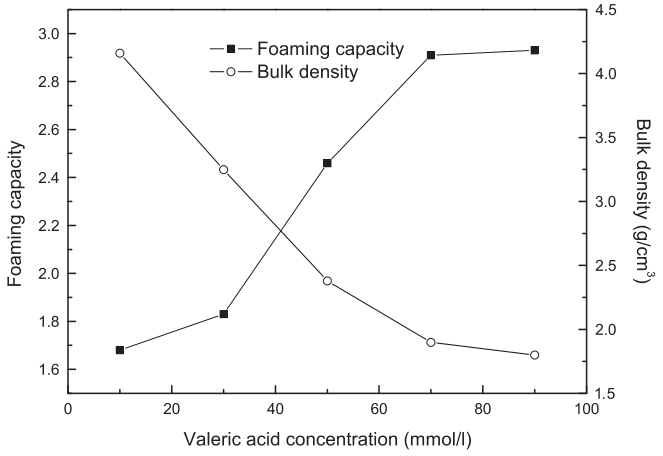


Fig. 1. Variations of foaming capacity and bulk density of porous PZT ceramics with valeric acid concentration (pH = 5).

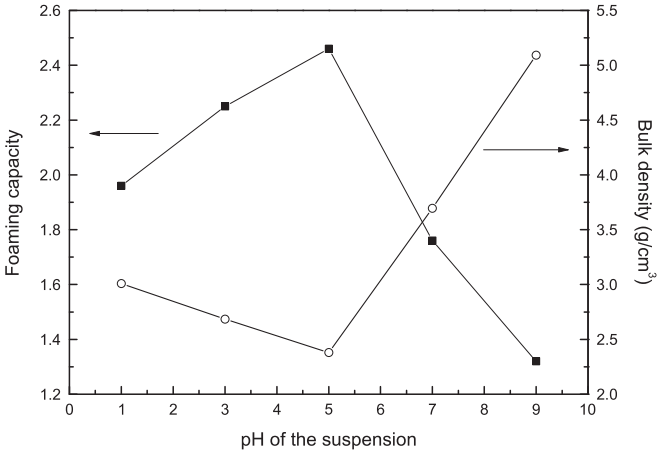


Fig. 2. Variations of foaming capacity and bulk density of porous PZT ceramics with pH value (valeric acid concentration = 50 mmol/L).

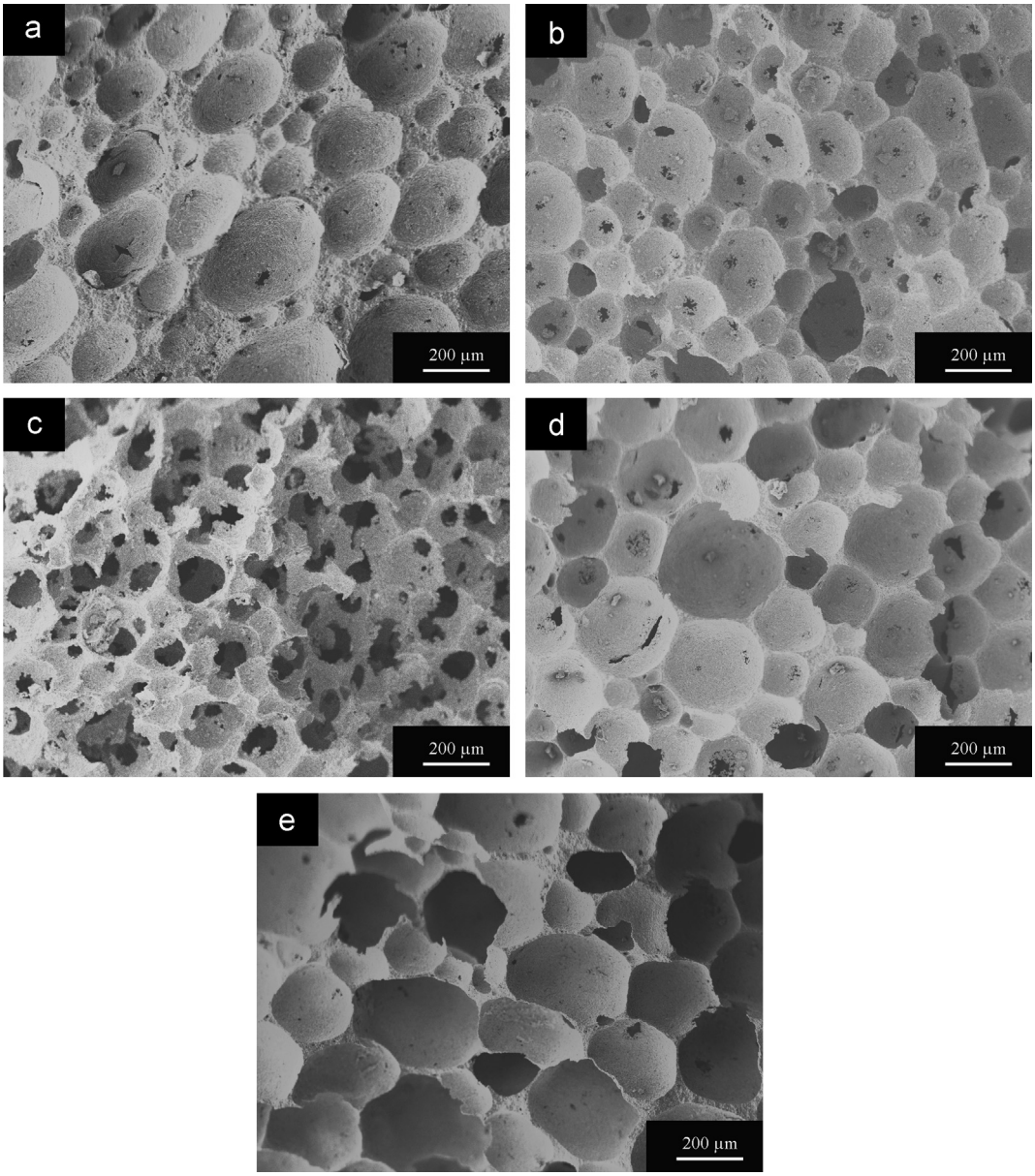


Fig. 3. SEM micrographs of porous piezoelectric materials with different valeric acid concentrations, pH values, and porosities: (a) 10 mmol/L, pH 5, 45.28%; (b) 50 mmol/L, pH 5, 68.70%; (c) 90 mmol/L, pH 5, 76.32%; (d) 50 mmol/L, pH 1, 60.42% and (e) 50 mmol/L, pH 9, 33.00%.

formation of closed cells. With increasing foaming capacity, the number of ceramic particles that constituted every unit of bubble coating decreased, so the holes began to appear on cell-wall for different shrinkages during the drying and sintering procedure. Therefore, pores with several tens of micrometers in size located within the internal wall of macroporous structures were formed with increasing porosity, as depicted in Fig. 3(b) and (c). Comparing with Fig. 3(b), (d), and (e), similar phenomena appeared as the open-cell structure turned to closed cell with the porosity of sintered ceramics decreasing from 68.7% (2.38 g/cm$^3$) to 33.0% (5.09 g/cm$^3$). Moreover, it is well known that air bubbles tend to reduce the total interfacial area through coalescence and disproportionation (Ostwald ripening), which definitely results in the collapse of wet foams and hence decrease in porosity of sintered specimens. Conversely, the decreasing foaming capacity should also imply the coarsening of cells, with the average size of cells being 137 μm, 170 μm, and 237 μm, respectively, as shown in Fig. 3(b), (d), and (e).

### 3.2. Dielectric property

Relative permittivity of porous PZT ceramics as a function of porosity is shown in Fig. 4. As discussed above, the sample with 68.7% porosity, which was prepared with suspensions containing 15 vol% PZT at pH 5 and 50 mmol/L valeric acid, was demonstrated in both Figs. 1 and 2 while discussing the effects of pH value and valeric acid concentration on the foaming capacity and bulk density of porous PZT ceramics. Therefore, while studying the effects of the two series of parameters on dielectric and piezoelectric properties, we demonstrated only one data point corresponding to 68.7%

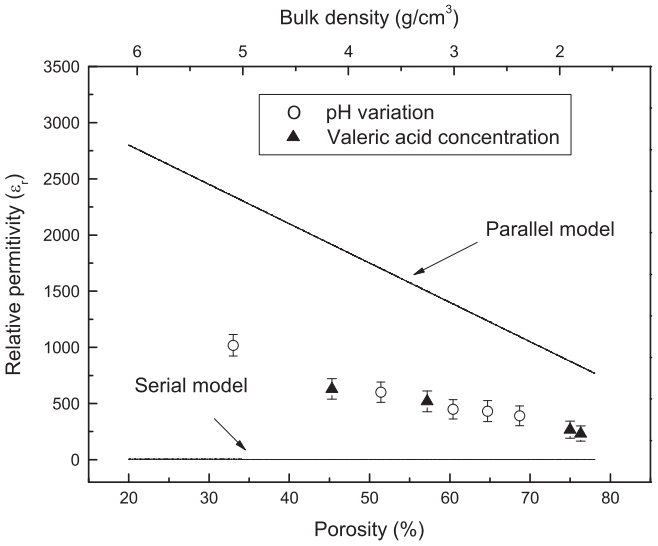


Fig. 4. Relative permittivity as a function of porosity.

porosity in relevant figures. As can be seen from Fig. 4, the relative permittivity decreased with the increasing porosity for all the specimens, which is consistent with previously reported results [19]. Meanwhile, porous ceramics can be regarded as a pore-solid composite whose dielectric property could be predicted by some theoretical models. In this study, the following general empirical equation was used to predict the relative permittivity of porous PZT ceramics:

$$\varepsilon_r^{\alpha} = \sum_i V_i \varepsilon_{ri}^{\alpha} \quad (2)$$

where $\varepsilon_r$ is the relative permittivity of porous materials, $V_i$ and $\varepsilon_{ri}$ are the volume fraction and relative permittivity of the $i$th material, respectively and $\alpha$ is a constant [20]. The value of the constant α is determined to be $\alpha=-1$ and $\alpha=1$ for serial and parallel mixing models, respectively. As shown in Fig. 4, the measured relative permittivity of porous PZT ceramics fell between the predictions of the serial and parallel mixing models. According to Zhang et al. [21], the parallel model predicts the $\varepsilon_r$ of porous PZT ceramics with closed cells, while the serial model is suitable for the high open-porosity ceramics. Obviously, both of the two models express two extreme cases of the mixing of two components. However, the measured value of $\varepsilon_r$ in low porosity was closer to that of the serial model, which did not match the empirical equation very well. We believe that besides the porosity, the measured $\varepsilon_r$ is also sensitive to the shape of pores in this study. This observation is consistent with the SEM micrographs in Fig. 3 that shows the irregular shape at low porosity.

### 3.3. Piezoelectric property

The correlation of longitudinal piezoelectric strain coefficient ($d_{33}$) with porosity is shown in Fig. 5. The $d_{33}$ values of porous PZT ceramics decreased almost linearly in the porosity range of 33.0–68.7%. According to the space-charge theory [22], the existence of pores brings about the increase of space-charge sites such as lattice vacancies or impurity atoms bounding inside grain boundaries; thus an increase in microscopic stress and strain emerges simultaneously, and reduces the piezoelectric coefficient by inhibiting the movement of domain walls in the end. When the porosity exceeded 68.7%, the $d_{33}$ value decreased drastically and it could be deduced that the increase of open cell affected the mechanical loadings seriously, and further lowered the piezoelectric coefficient.

Fig. 6 shows the hydrostatic strain coefficient ($d_h$) as a function of porosity. As to the variation of pH values, the $d_h$ value increased from 178 to 209 pC/N with the porosity ranging from 33.0% to 68.7%. Apparently, the faster descending trend of $d_{31}$ value than that of $d_{33}$ led to the ascending trend of $d_h$ values with increasing porosity. However, the effect of valeric acid concentration on $d_h$ values shows different trends. Firstly, when the porosity ranged from 45.3% to 75.0%, the $d_h$ value increased from 179 to 212 pC/N remarkably. Then the $d_h$ value decreased to 200 pC/N with the porosity of 76.3%. It is believed that the interconnecting pores in specimen with high open porosity (Fig. 3 (c)) made

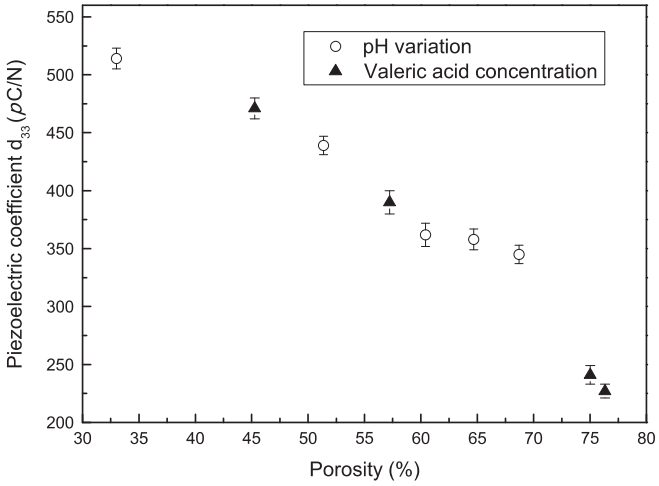


Fig. 5. Variation of longitudinal piezoelectric strain coefficient ($d_{33}$) values with porosity.

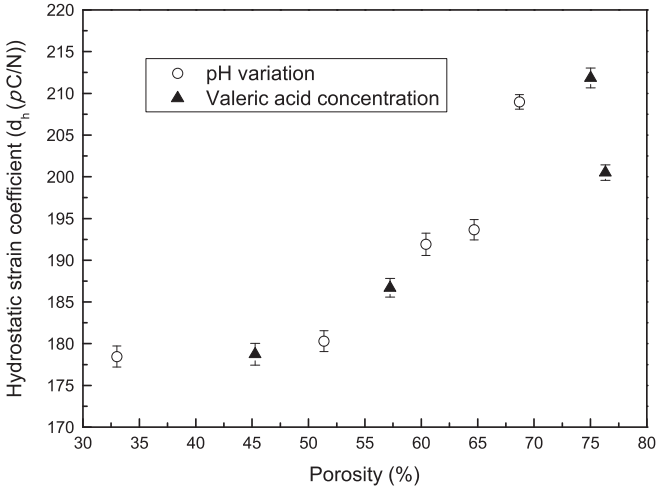


Fig. 6. Hydrostatic strain coefficient ($d_h$) as a function of porosity.

the $d_{33}$ value decrease at a more rapid rate than that of $d_{31}$, so the $d_h$ value decreased appropriately.

With the increase of porosity, the lowered $\varepsilon_r$ and high value of $d_h$ led to promoted value of hydrostatic voltage coefficient ($g_h$), and hence hydrostatic figure of merit (HFOM) with respect to dense PZT ceramics. As can be seen from Fig. 7, no matter how the compositions of suspension changed, the HFOM increased obviously with the increase of porosity with the highest value of $19{,}520 \times 10^{-15}$ Pa$^{-1}$, much higher than that of previous research [23]. However, the low value of $\varepsilon_r$ corresponding to high porosity is always harmful for the stability and reliability of specimen. The capacitance, $C$, which characterizes the stability of specimen, could be calculated from the inversion formula

$$C = \varepsilon_r \varepsilon_0 \frac{S}{d} \tag{3}$$

Apparently, the high value of HFOM with high porosity suggests a low value of $C$. Therefore, a compromise should be made when deciding the composition of final suspension to achieve optimum values of piezoelectric properties and relative permittivity simultaneously.

### 3.4. Acoustic impedance

Fig. 8 shows the acoustic impedance of porous PZT ceramics as a function of porosity. The acoustic impedance, $Z$, could be calculated by the following formula:

$$Z = \rho_m D f_r \tag{4}$$

where $\rho_m$ is the measured density of porous PZT ceramics, $D$ is the diameter of the disc-shaped specimen, and $f_r$ is the resonant vibration frequency. As shown in Fig. 8, the $Z$ values decreased almost linearly from 6.53 to 1.35 Mrayl with increasing porosity due to the gradual introduction of air filled pores into the ceramic matrix. The lowest value of $Z$ was close to that of biological tissue (1–2 Mrayl) or water (~1.5 Mrayl), which is beneficial in improving acoustic matching and helpful for ultrasonic transducers application like hydrophone or medical imaging. Meanwhile, there is no apparent discrepancy in the dependence of acoustic impedance on porosity, which

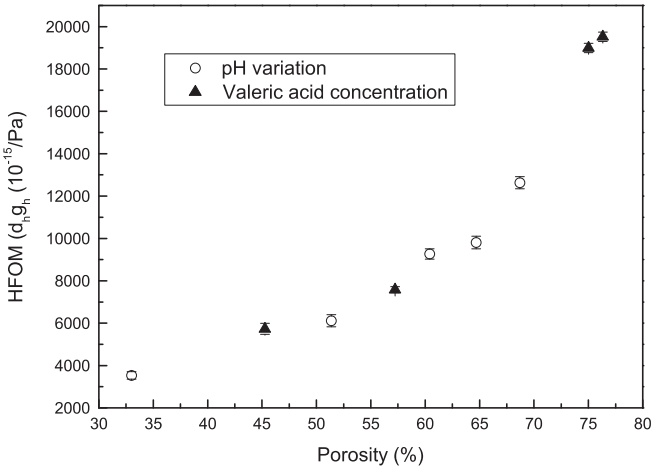


Fig. 7. Variation of hydrostatic figure of merit (HFOM) with porosity.

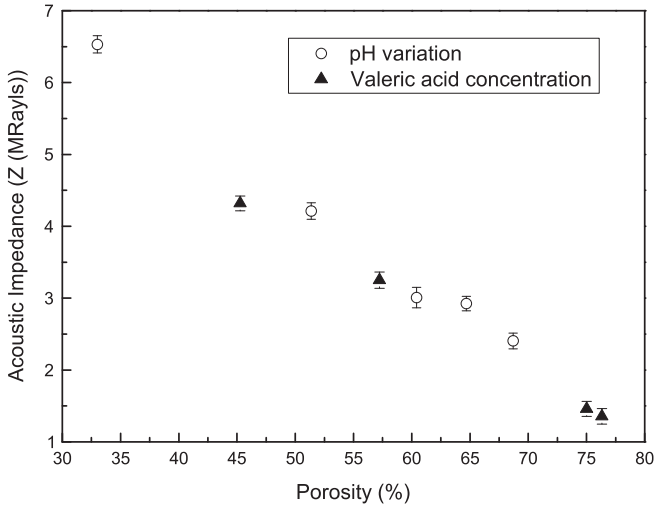


Fig. 8. Acoustic impedance as a function of porosity.

suggests that the acoustic impedance of porous PZT ceramics in this study is sensitive mainly to porosity, not to the shape or connectivity of pores.

## 4. Conclusion

In this work, particle-stabilized foams and the gelcasting technique were combined to produce porous PZT ceramics. By varying the concentrations of valeric acid and pH values of final suspension, wet foams with different foaming capacities were prepared, while the porosity and microstructure of sintered specimens changed accordingly. As for the dielectric and piezoelectric properties, the values of $\varepsilon_r$ and $d_{33}$ of porous PZT ceramics not only decreased with increasing porosity, but also were affected by the shape or structure of pores. The value of $d_h$ increased moderately with the increase of porosity, which allowed the porous PZT ceramics to have high HFOM values. The sample with a porosity of 76.3% showed a HFOM value of as high as $19520 \times 10^{-15}$ Pa$^{-1}$. The acoustic impedance decreased almost linearly with increasing porosity, and reached the lowest value of 1.35 Mrayl, so the porous material of this kind is suitable for the design of underwater hydrophone.

## Acknowledgment

Our research work presented in this article is supported by Innovation Method Special Project of Ministry of Science and Technology of China (Grant no. 2011IM030800), and the National Natural Science Foundation of China (Grant nos. 51172120 and 51102216). The authors are grateful for these grants.

## References

[1] C.R. Bowen, V.Y. Topolov, Piezoelectric sensitivity of $PbTiO_3$-based ceramic/polymer composites with 0–3 and 3–3 connectivity, Acta Materialia 51 (2003) 4965–4976.

[2] K.S. Challagulla, T.A. Venkatesh, Electromechanical response of piezoelectric foams, Acta Materialia 60 (2012) 2111–2127.

[3] R. Guo, C.A. Wang, A.K. Yang, Effects of pore size and orientation on dielectric and piezoelectric properties of 1–3 type porous PZT ceramics, Journal of the European Ceramic Society 31 (2011) 605–609.
[4] C. Galassi, Processing of porous ceramics: piezoelectric materials, Journal of the European Ceramic Society 26 (2006) 2951–2958.
[5] D.P. Skinner, R.E. Newnham, L.E. Cross, Flexible composite transducers, Materials Research Bulletin 13 (1978) 599–607.
[6] S.S. Livneh, V.F. Janas, A. Safari, Development of fine scale PZT ceramic fiber/polymer shell composite transducers, Journal of the American Ceramic Society 78 (1995) 1900–1906.
[7] Z.M He, J. Ma, R.F. Zhang, Investigation on the microstructure and ferroelectric properties of porous PZT ceramics, Ceramics International 30 (2004) 1353–1356.
[8] A.K. Yang, C.A. Wang, R. Guo, Y. Huang, Effects of porosity on dielectric and piezoelectric properties of porous lead zirconate titanate ceramics, Applied Physics Letters 98 (2011) 152904.
[9] A.R. Studart, U.T. Gonzenbach, E. Tervoort, L.J. Gauckler, Processing routes to macroporous ceramics: a review, Journal of the American Ceramic Society 89 (2006) 1771–1789.
[10] U.T. Gonzenbach, A.R. Studart, E. Tervoort, L.J. Gauckler, Macroporous ceramics from particle-stabilized wet foams, Journal of the American Ceramic Society 90 (2007) 16–22.
[11] U.T. Gonzenbach, A.R. Studart, E. Tervoort, L.J. Gauckler, Ultrastable particle-stabilized foams, Angewandte Chemie International Edition 45 (2006) 3526–3530.
[12] A.C. Young, O.O. Omatete, M.A. Janney, P.A. Menchhofer, Gelcasting of alumina, Journal of the American Ceramic Society 74 (1991) 612–618.
[13] O.O. Omatete, M.A. Janney, S.D. Nunn, Gelcasting: from laboratory development toward industrial production, Journal of the European Ceramic Society 17 (1997) 407–413.
[14] J.L. Yu, J.L. Yang, Y. Huang, The transformation mechanism from suspension to green body and the development of colloidal forming, Ceramics International 37 (2011) 1435–1451.
[15] R.F. Chen, Y. Huang, C.A. Wang, J.Q. Qi, Ceramics with ultra-low density fabricated by gelcasting: an unconventional view, Journal of the American Ceramic Society 90 (2007) 3424–3429.
[16] W. Liu, J. Xu, Y.Z. Wang, H. Xu, X.Q. Xi, J.L. Yang, Processing and properties of porous PZT ceramics from particle stabilized foams via gelcasting, Journal of the American Ceramic Society, http://dx.doi.org/10.1111/jace.12250
[17] W.S. Rasband, ImageJ, 1997–2009, ⟨http://rsb.info.nih.gov/ij/⟩.
[18] A. Navarro, J.R. Alcock, R.W. Whatmore, Aqueous colloidal processing and green sheet properties of lead zirconate titanate (PZT) ceramics made by tape casting, Journal of the European Ceramic Society 24 (2004) 1073–1076.
[19] A.K. Yang, C.A. Wang, R. Guo, Y. Huang, C.W. Nan, Porous PZT ceramics with high hydrostatic figure of merit and low acoustic impedance by TBA-based gel-casting process, Journal of the American Ceramic Society 93 (2010) 1427–1431.
[20] K. Wakino, T. Okada, N. Yoshida, K. Tomono, A new equation for predicting the dielectric constant of a mixture, Journal of the American Ceramic Society 76 (1993) 2588–2594.
[21] H.L. Zhang, J.-F. Li, B.P. Zhang, Microstructure and electrical properties of porous PZT ceramics derived from different pore-forming agents, Acta Materialia 55 (2007) 171–181.
[22] K. Okazaki, K. Nagata, Effects of grain size and porosity on electrical and optical properties of PLZT ceramics, Journal of the American Ceramic Society 56 (1973) 82–86.
[23] A.K. Yang, C.A. Wang, R. Guo, Y. Huang, Microstructure and electrical properties of porous PZT ceramics fabricated by different methods, Journal of the American Ceramic Society 93 (2010) 1984–1990.